CHAPTER 1

Concentrated O/W Emulsions Stabilized by Proteins: A Route to Texturize Vegetal Oils Without Using Trans *or Saturated Fats*

W. DRIDI,[a] R. KAPEL,[b] S. ALBE-SLABI[b] AND F. LEAL-CALDERON*[a]

[a] Université de Bordeaux, CNRS, Bordeaux INP, CBMN UMR 5248, 33600, Pessac, France; [b] Laboratoire Réactions et Génie des Procédés, Université de Lorraine, CNRS, LRGP, 54000 Nancy, France
*Email: fleal@enscbp.fr

1.1 Introduction

Public health and sustainable development objectives induce a pressing need for the substitution of saturated fats. Palm oil (PO) has been widely used owing to its advantageous features: texturizing ability linked to its solid-like behavior at room temperature, chemical stability, and high oil yield per hectare. The demand for PO has increased over recent decades, which has had profound consequences for the environment in terms of deforestation, land tenure, and community conflicts in countries where it is cultivated. This issue has led to the so-called ''Roundtable on Sustainable

Food Chemistry, Function and Analysis No. 31
Development of *Trans*-free Lipid Systems and their Use in Food Products
Edited by Jorge F. Toro-Vazquez

Published by the Royal Society of Chemistry, www.rsc.org

Palm Oil'' (RSPO) certification system, whose guidelines are sometimes considered insufficiently restrictive and are not always respected.

The interesting properties of PO are linked to its composition rich in saturated fatty acids (SFAs). Many countries are not PO producers but they produce vegetable oils from rapeseed or sunflower. One alternative to PO consists of submitting vegetable oils to hydrogenation. However, this process may induce the formation of *trans* double-bonds that have harmful effects on human health. In particular, they have a negative impact on the plasma lipoprotein profile as they increase the level of LDL (Low Density Lipoproteins, ''bad cholesterol'') and lower the level of HDL (High Density Lipoproteins, ''good cholesterol''). Studies show that a daily intake of *trans*-fatty acid chains (TFACs) larger than 2% of the total energy intake (TEA) significantly increases the prevalence of cardiovascular diseases, which represent the major proportion of non-communicable diseases (40%), ahead of cancer (27%).[1] The World Health Organization (WHO) recommends limiting consumption of SFAs to 10% and that of TFACs to 2% of the TEA. As a matter of fact, WHO already foresees complete elimination of industrial TFACs.[2]

In this context, food grade systems based on liquid vegetal oils and exhibiting the rheological properties of soft solids are highly sought after. To achieve this goal, two different strategies can be envisaged. The first one consists of introducing compounds which are partially insoluble in oil. Very often, this involves crystallizing triacyglycerides rich in saturated long chains and aggregating the microcrystals to form fractal structures.[3] Other organogel-like systems consist of self-assemblies into long nanotubes that form a 3D entangled network.[4] The second strategy consists of forming oil-in-water (O/W) concentrated emulsions. For instance, Patel *et al.*[5] proposed an emulsion-templated approach for the preparation of oleogels by using a combination of a surface-active and a non-surface-active polysaccharide. The oleogels were prepared *via* a two-step process: (1) formulation of a concentrated O/W emulsion stabilized with a combination of cellulose derivatives and xanthan gum, and (2) selective evaporation of the continuous water phase to drive network formation. An analogous strategy will be considered in the present study, but using solely proteins to stabilize the emulsions. Our approach aims at conferring viscoelastic properties to liquid oils through the interfaces that oil droplets form with the aqueous phase. Texturizing will result from the emulsification of oil in water by vegetable proteins that adsorb at the oil/water interface, followed by droplet concentration through centrifugation or water evaporation.

At low volume fractions, emulsions comprise spherical droplets and behave like viscous fluids. Owing to droplet deformation, emulsions may be concentrated up to volume fractions much higher than the volume fraction corresponding to the close packing of a dispersion of hard spheres, ϕ^*. For randomly monodisperse spheres, $\phi^* \approx 64$ vol%. Above ϕ^*, the droplets can no longer pack without deforming. Emulsions then become predominantly solid at low deformations and exhibit considerable yield stress. As stated by Princen[6] and Mason *et al.*,[7] the elasticity (solid-like behavior) of concentrated emulsions is due to droplets that have been compressed by the application of

an external osmotic pressure, Π. Actually, emulsions minimize their free energy by reducing droplet repulsion at the expense of deforming the droplet interfaces at each contact (films become flat), which creates additional surface area. The osmotic pressure Π is the energy per unit volume required to deform the droplets up to a volume fraction ϕ. Additional excess surface area created by a perturbative strain or stress determines the elastic shear modulus, G'. Although Π and G' represent different properties, they both depend on the degree of droplet deformation and therefore on ϕ.

In this study, we explored pathways to obtain very viscous fluids and highly elastic pastes by exploiting the intrinsic properties of concentrated emulsions. We used as emulsion stabilizers proteins extracted from by-products of the oil industry, namely press-cakes. These by-products were selected because they are abundant and have a large protein content. It has been established that in emulsions at droplet volume fractions above ϕ^*, both the elastic and viscous moduli (G' and G'') increase as the droplet radius decreases.[7] Conditions were thus adopted so as to minimize the droplet radius. Dilute emulsions of various average droplet diameters were first fabricated. We used high pressure homogenization coupled with the so-called limited coalescence process, at low protein content, to produce fine emulsions (average diameter <5 μm) with narrow size distributions.[8] The initially dilute emulsions were concentrated by centrifugation and evaporation. The osmotic compressibility, Π, was measured for two average droplet sizes and variable volume fractions above the random close packing, ϕ^*. The dimensionless osmotic compressibility $\Pi(\phi)/(\gamma/R)$, where R is the average droplet diameter and γ is the oil/water interfacial tension, was compared to that obtained in previous studies for equivalent surfactant-stabilized emulsions. Finally, we explored the possibility to fabricate redispersible dry-emulsion powders through a freeze-drying process.

1.2 Experimental

1.2.1 Materials

Rapeseed oil (density $= 0.916$ g cm^{-3} at 20 °C) was purchased from a local supermarket. All other reagents were from Aldrich. Hexadecane (density $= 0.773$ g cm^{-3} at 20 °C) was the oil phase in model systems. NaN_3 at a concentration of 0.01 mol L^{-1} was incorporated in all aqueous phases to prevent bacterial growth. Bradford reagent was used for protein quantification. Sodium dodecyl sulfate (SDS) helped to deflocculate emulsions during droplet size measurements. Different saccharides were probed as wall materials to protect emulsions from coalescence during the lyophilization step: Lactose ($C_{12}H_{22}O_{11}$), mannitol ($C_6H_{14}O_6$), and trehalose ($C_{12}H_{22}O_{11}$).

1.2.2 Sunflower Protein Isolate

All emulsions were fabricated with a sunflower protein (SP) isolate obtained from an industrial sunflower press-cake, made up of about 30% proteins, the

two main families of which are globulins and albumins. Isolates contain 40 to 90% of globulins and 10 to 30% of albumins, depending on the variety of sunflower.[9] The remaining protein fractions are composed of prolamins, glutelins, and free polypeptide segments.

SP extraction was performed using a one liter reactor stirred at 400 rpm. The appropriate amount of cake and a 1 mol L^{-1} NaCl aqueous phase were added in order to obtain a 1 : 9 w/w (solid/liquid) mixture. A solution at 1 mol L^{-1} NaOH was used to adjust and maintain the pH at 7. The mixture was processed in the reactor at room temperature, for 30 min. Solid–liquid separation was carried out by centrifugation at 15 000 g (with g being the earth gravity constant), at room temperature for 30 min. The aqueous phase was filtered through pleated cellulose filters (Fisherbrand, France). During this step, sunflower albumins and globulins were extracted as well as other water-soluble compounds (free phenolics, oses, osides, amino acids, and free peptides). These compounds were removed by an ultrafiltration process. This process began with a diafiltration step on an Akta flux® 6 ultrafiltration pilot (GE Healthcare, USA) coupled with a 3 kDa cut-off, 4800 cm^2 hollow fiber. First, the liquid extract was concentrated by a 4.2 volume reduction factor, and the retentate was washed with 6 diafiltration volumes (DV) of 0.5 mol L^{-1} NaCl. Then, the pH was adjusted to 10 using a solution of 1 mol L^{-1} NaOH, and the retentate was washed additionally with 4 DV of ultrapure water. The final retentate was collected and freeze-dried. The sunflower isolate was analyzed by the Kjeldahl method[10] to determine its protein content. The obtained sample contained 91 wt% of proteins on a dry matter basis.

In order to determine the protein nature, the isolate was analyzed by high pressure liquid chromatography (HPLC, LC20 system from Shimadzu, Japan) and polyacrylamide gel electrophoresis in the presence of sodium dodecyl sulfate (SDS-PAGE). To perform chromatography, 10 μL of protein isolate solution at the concentration of 5 g L^{-1} were injected into a Biosep SEC s-2000 column (300×7.8 mm; 5 μm; Phenomenex, USA) and eluted using an acetonitrile/ultrapure water/trifluoroacetic acid (45 : 54.9 : 0.1 v/v) mixture flowing at 0.6 mL min^{-1}. Optical detection was performed at the wavelength $\lambda = 280$ nm.[11] Figure 1.1A shows the obtained chromatogram. The dotted lines represent the limits of the areas corresponding to globulins and albumins. Based on these areas and knowing the total protein content, it was possible to estimate the proportion of globulins and albumins in the isolate. Since the two peaks overlapped slightly, the area ratio only provides an estimate. The area corresponding to globulins is considered to be that under the curve at elution times between 8.0 min and 10.2 min, and the area corresponding to albumins is that between 10.2 min and 12.8 min. We deduce that the isolate is composed of 82% globulins and 18% albumins.

An SDS-PAGE technique under reducing conditions was used to confirm that the peaks correspond to sunflower globulins and albumins. For this purpose, a protein solution at a concentration of 5 g L^{-1} was diluted in 50 μL of Laemmli buffer containing 2% β-mercaptoethanol (v/v) and then heated at 95 °C over 5 min. Proteins were separated in a gel composed of 5% stacking and 17%

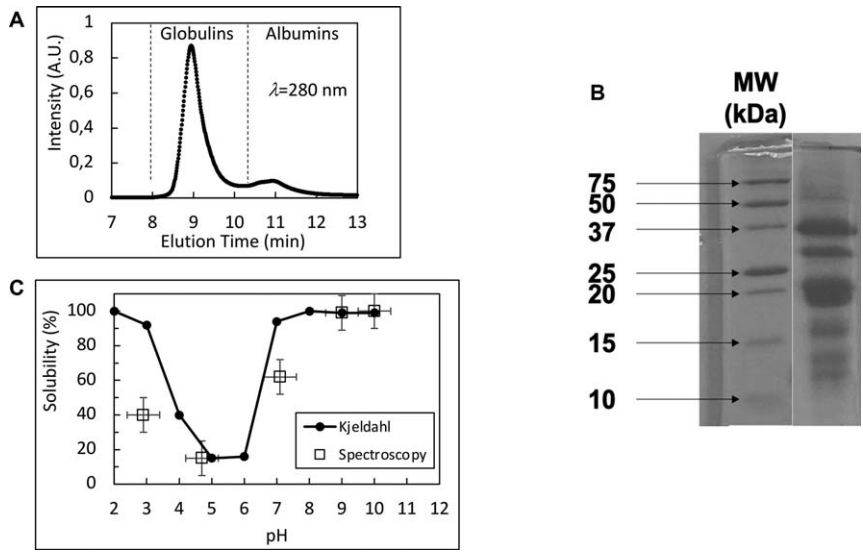

Figure 1.1 (A) HPLC chromatogram of the sunflower protein isolate measured at $\lambda = 280$ nm; (B) SDS-PAGE electrophoresis patterns of the protein isolate; (C) Protein solubility as a function of pH measured by the Kjeldahl method and UV-spectroscopy.

resolving gel by applying an electric current of 20 mA. A Precision Plus Protein Standard (10–250 kDa from Bio-Rad, USA) was used as a molecular weight marker. After migration, gels were stained with Coomassie Brilliant Blue and destained overnight in a 10% acetic acid solution (v/v). The obtained electrophoresis pattern is reported in Figure 1.1B. The left-hand side pattern was obtained with molecular weight markers to define the position scale. The right-hand side pattern is that of the whole isolate sample. The molar mass at 50 kDa is that of sunflower globulin monomer which is hexameric in its native state; the masses between 26 and 37 kDa correspond to acid polypeptides and those between 18 and 25 kDa to the basic polypeptides.[12–14] The molar masses from 14 to 18 kDa can be attributed to sunflower albumins.[15–17]

The solubility of the isolate as a function of pH was determined by two methods.

(i) The isolate was dispersed in reverse osmosis water at 5 $g\,L^{-1}$. pH adjustment was made by adding small volumes of 1 $mol\,L^{-1}$ solutions of HCl and NaOH. The mixture was stirred for 20 min and then centrifuged (11 000 g, 20 min, 20 °C). The concentration of proteins in the supernatant was measured by the Kjeldahl method.[10]

(ii) The solubility as a function of pH was also determined by UV-spectrometry. Measurements were carried out at the same ionic strength of 0.1 $mol\,l^{-1}$, at pH 3 (acetate buffer), 5 (citrate buffer), 7 (phosphate buffer), and 10 (buffer carbonate).

The plots in Figure 1.1C show that the measured solubility is the same for the two protocols, except for the citrate buffer solution at pH 3, which appears to reduce solubility more than a hydrochloric acid solution at the same pH. As citric acid is a poly-anion, it is able to complex a fraction of the proteins. Full solubility of the sunflower isolate is obtained at $pH > 7$ and in highly acidic conditions ($pH < 2$). The solubility dip observed at $4 < pH < 6$ is due to the isoelectric point of the proteins.[18]

The hydrodynamic radius of the proteins was characterized by dynamic light-scattering (Amtec goniometer (France) and Brookhaven BT9000 correlator (USA)) performed at a wavelength $\lambda = 532$ nm for different scattering angles between 40 and 120° with respect to the incident beam, at 20 °C.[19] The protein solutions were filtered through an ester cellulose filter (CME 0.22 mm, Karl Roth, Germany). The hydrodynamic radius deduced from the diffusion coefficient was $R_h = 10 \pm 1$ nm. This value also obtained by other authors[20] roughly corresponds to the dimension of globulin hexamers.[21]

1.2.3 Methodologies

1.2.3.1 Emulsion Preparation

Both hexadecane-in-water and rapeseed oil-in-water emulsions stabilized by sunflower proteins were prepared. Hexadecane was adopted as a model system in a series of experiments because of its high purity and chemical inertness, allowing a precise determination of the oil/water interfacial tension without artifacts linked to triglyceride hydrolysis. It was also used to generalize the concepts and to provide evidence that the main properties of concentrated emulsions are determined, not by the chemical nature of the oil phase, but by the interfacial properties.

O/W emulsions were prepared using a two-step procedure. First, 25 g of a coarse emulsion at 20 wt% of oil were fabricated using an Ultra-turrax® T-25 disperser (IKA, Germany) operating at 3000 rpm for 5 min. The aqueous phase contained SP from the isolate at a concentration from 0.25 to 2 wt%, and the pH varied between 8.5 and 9.2. This basic pH was due to the presence of NaOH from the extraction process. This pH assured full SP solubilization, as described in Section 1.2.2. The coarse emulsions were then submitted to a second homogenization step using a microfluidizer (Microfluidics M110S, Massachusetts, USA) at a pressure of 800 bars. Emulsions underwent 8 passes through the homogenizing chamber. To avoid sample warming, the emulsions passed through a metallic coil immersed in a cold-water bath (8 °C). Through this procedure, the emulsions obtained at the end of the emulsification process were close to room temperature.

1.2.3.2 Emulsion Characterization

Oil droplets were observed after emulsification and as a function of time using an optical microscope Olympus BX51 (Olympus, Germany) equipped

with a digital camera (Leica, 2576×1932-pixel resolution, Germany). The droplet size distributions were measured by static light-scattering, using a Mastersizer 2000 Hydro SM from Malvern Instruments S.A (UK). The droplet size distributions were characterized in terms of their surface-averaged diameter, d_{32}, and polydispersity, P, defined as:

$$d_{32} = \frac{\sum N_i D_i^3}{\sum N_i D_i^2}, \quad P = \frac{1}{\bar{D}} \frac{\sum N_i D_i^3 (\bar{D} - D_i)}{\sum N_i D_i^3} \tag{1.1}$$

where $\bar{D}$ is the median diameter, *i.e.,* the value for which the cumulative undersized volume fraction is equal to 50%, and N_i is the total number of droplets with diameter D_i. Static light-scattering data were transformed into droplet size distribution using Mie theory.[22] The refractive index adopted for calculations was 1.43 for hexadecane, 1.47 for rapeseed oil, and 1.33 for water. Before analysis, emulsions underwent a 10-fold dilution in a 1 wt% SDS solution to disaggregate the droplets. The measuring cell was filled with pure water, and a small volume of the emulsion was introduced under stirring (1400 rpm).

1.2.3.3 Protein Quantification

After emulsification, a fraction of the proteins initially dissolved in the aqueous phase was irreversibly adsorbed at the oil/water interface. The residual protein concentration in the aqueous phase was measured using the Bradford assay.[23] The emulsions were centrifuged for 10 to 20 min at accelerations between 1000 *g* and 10 000 *g* (Eppendorf Centrifuge 5430, Germany). Under the effect of buoyancy, a cream of oil droplets was formed at the top of the centrifuge tube. The protein concentration in the subnatant, $C_{\mathrm{Pr}}^{\mathrm{f}}$, was measured, and the mass of proteins adsorbed at the interface, m_{a}, was determined by considering the following mass balance:

$$m_{\mathrm{a}} = (C_{\mathrm{Pr}}^{0} - C_{\mathrm{Pr}}^{\mathrm{f}}) V_{\mathrm{aq}} \tag{1.2}$$

where C_{Pr}^{0} is the protein concentration in the aqueous phase before emulsification, and V_{aq} is the volume of the aqueous phase.

1.2.3.4 Osmotic Pressure Measurements

Emulsions were concentrated by centrifugation using a Beckman Coulter (Avanti J-30I JS-24.15, USA) centrifuge equipped with JS-24.15 Swinging-Bucket Aluminum Rotor. Emulsions were processed for a time ranging from 90 min to 5 hours at accelerations from 1000 g to 100 000 g. Centrifugation was applied until constant droplet volume fraction was achieved in the cream. After creaming, if the thickness of the cream formed by the droplets is much lower than the length of the centrifuge lever arm, the spatial gradient in the acceleration can be neglected, and the osmotic pressure can be determined as:[24]

$$\Pi = L \Delta\rho \omega^2 \phi_i d \tag{1.3}$$

where L is the total liquid height in the centrifuge tube, ϕ_i is the initial oil volume fraction before centrifugation, $\Delta\rho$ is the density mismatch between oil and water, d is the length of the lever arm, and ω is the rotation speed of the centrifuge.

A small amount of the cream located at the top of the centrifugation tube was collected and left in a dry place at room temperature for approximately 12 h. During this time period, hexadecane evaporation was confirmed to be negligible due to its very low volatility. Samples weighing before and after water evaporation provided a direct measure of the oil volume fraction, ϕ.

1.2.3.5 Interfacial Tension

The oil/water interfacial tension γ was measured using the rising drop method (Tracker apparatus, Teclis Instruments, France). A droplet of hexadecane (10 μL) was formed at the tip of a steel needle in a transparent cell filled with an aqueous phase containing 0.2 $g\,L^{-1}$ of SP, at pH 8.2. Images of the droplets were recorded at regular time intervals with a digital camera. The droplet profile was analyzed to calculate its area and surface tension by solving the Laplace–Young equation. The oil/water interfacial tension decreased over time until reaching an asymptotic value of 15 $mN\,m^{-1}$ that will be used in further calculations.

1.2.3.6 Emulsion Drying

The emulsions were dried by lyophilization right after preparation. They were stored at least 12 h at −80 °C and then introduced into a freeze-dryer (FTS Systems, Dura-Dry, USA) at a pressure of 0.1 mbar for 24 h. The residual moisture in the powders was determined with a moisture analyzer (Ohaus MB120, USA). The obtained powders were stored at room temperature.

1.2.3.7 Redispersion of Dried Emulsions

The powders were gently redispersed by vigorous manual mixing for 1 min, until the samples became homogeneous, with the amount of distilled water required to restore the same composition as that of the parent emulsions. Their size distribution was measured after redispersion following the method described in Section 1.2.3.2.

1.3 Results and Discussion

1.3.1 Impact of the Protein Content on the Average Droplet Size

Hereafter, SP concentrations will be expressed in weight percent of the aqueous phase. Emulsions containing variable amounts of SP, from 0.25 to 2 wt%, were prepared. The data in Figure 1.2 were obtained for a hexadecane-in-water emulsion containing 1 wt% of SP. The emulsion was

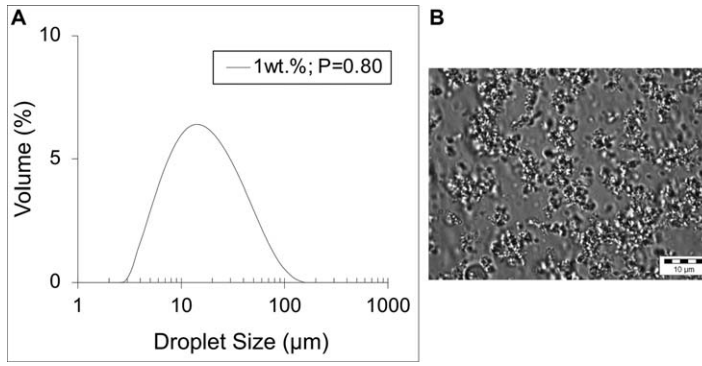

Figure 1.2 (A) Droplet size distribution of a hexadecane-in-water emulsion initially containing 1 wt% sunflower protein in the aqueous phase. Measurements were performed right after emulsification. (B) Micrograph of the same emulsion. Samples were analyzed without prior dilution in an SDS solution.

first analyzed by diluting it in pure water. The size distribution in Figure 1.2A is wide, as reflected by the relatively high value of the polydispersity index ($P = 0.8$). Actually, the size distribution does not reflect the size of individual droplets but that of droplet aggregates. Indeed, the micrograph of Figure 1.2B shows that all droplets are immobilized within large ramified clusters. The same aggregated state was obtained, irrespective of the oil nature (rapeseed oil or hexadecane) and of the protein content.

It is well known that the presence of SDS can disrupt protein aggregates and deflocculate emulsions. This is evidenced in the micrograph of Figure 1.3B, corresponding to an emulsion based on hexadecane, containing 0.25 wt% of SP. Prior to its observation under the microscope and analysis by light-scattering, the emulsions were diluted with a 1 wt% SDS solution. In this case, individual droplets submitted to Brownian motion are observed, and the size distributions reported in Figure 1.3A are quite narrow, with P values being lower than 0.40. Interestingly, the distribution shifts toward lower sizes as the protein concentration increases. The protein concentrations explored here are rather low, and it is likely that the shear applied by the microfluidizer is able to generate much more interfacial area than the proteins can cover. Since proteins are in general irreversibly adsorbed, conditions are thus met for the so-called limited coalescence process to occur: when the agitation is stopped, droplets recombine until the degree of interfacial coverage becomes sufficient to stabilize them against further coalescence. One of the main features of limited coalescence is its ability to generate narrow droplet size distributions.[8]

1.3.2 Interfacial Coverage

The total droplets interfacial area, A, can be expressed as:[8]

$$A = \frac{6V_d}{d_{32}} = \frac{m_a}{\Gamma} \tag{1.4}$$

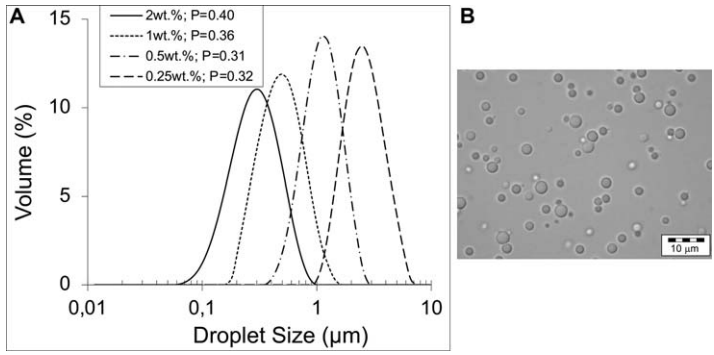

Figure 1.3 (A) Droplet size distribution of a hexadecane-in-water emulsion as a function of the initial sunflower protein concentration in the aqueous phase, expressed in weight percent of the aqueous phase. The initial sunflower protein concentrations varied from 0.25 wt% to 2 wt%. (B) Micrograph of the emulsion obtained with 0.25 wt% sunflower protein. Emulsions were diluted in a 1 wt% SDS solution before analysis.

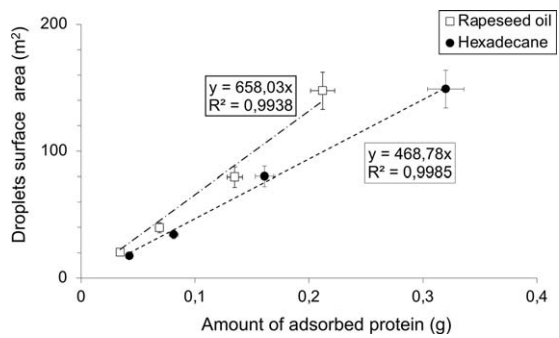

Figure 1.4 Droplet surface area as a function of the mass of sunflower protein adsorbed for emulsions with 20 wt% hexadecane or rapeseed oil. The total emulsion mass was 25 g.

where V_d is the volume of the dispersed phase and m_a is given by eqn (1.2). Assuming that the interfacial coverage adopts a unique value at the end of the limited coalescence process, Γ can be determined from the slope of the curve representing the evolution of the total surface area of the droplets, A, as a function of m_a. Figure 1.4 shows the corresponding plot. The linearity confirms the hypothesis about the existence of a unique interfacial coverage right after the emulsification process. From the slope, we deduce $\Gamma = 2.1 \pm 0.1$ mg m^{-2} and 1.5 ± 0.1 mg m^{-2} for emulsions based on hexadecane and on rapeseed oil, respectively. The emulsions were kinetically stable, with no apparent evolution of their size distributions over a time storage period of at least one month, at room temperature.

1.3.3 Emulsions Concentrated by Centrifugation – Osmotic Resistance Measurements

The emulsions based on hexadecane with average diameters $d_{32} = 0.24$ μm and 0.49 μm were centrifuged following the method described in Section 1.2.3.4 in order to obtain the Π *vs.* ϕ curves. Within the experimental conditions adopted, ϕ values from 65% to 95 vol% were obtained. The size distributions of the concentrated emulsions were identical to the initial ones (data not shown). In Figure 1.5A, we report the experimental data obtained for the two average droplet diameters. We would like to emphasize that the experimental points in our case refer to $\Pi(\phi)$ curves which are only valid for compression. Indeed, compressed emulsions did not redisperse spontaneously, even after being in contact with a large quantity of aqueous phase for a week. The compaction process probably involves some irreversibility. Since our emulsions did not expand when the applied pressure was set to zero, hereafter, the parameter Π defined by eqn (1.3) will be termed ''osmotic resistance''.

It is instructive to plot the data in $\Pi/(\gamma/R)$ with $R = d_{32}/2$, *versus* ϕ coordinates: this type of plot provides a possibility to compare the results with literature data excluding the effects of droplet size and interfacial tension. The first quantitative study on the properties of monodisperse emulsions was performed by Mason *et al.*[7] They investigated silicon O/W emulsions stabilized by SDS with different average diameters. The elastic shear modulus G' and the osmotic pressure Π had comparable values and were found to increase by nearly 4 decades as the droplet fraction, ϕ, increased from 50 to approximately 90 vol%. They both exhibited a universal

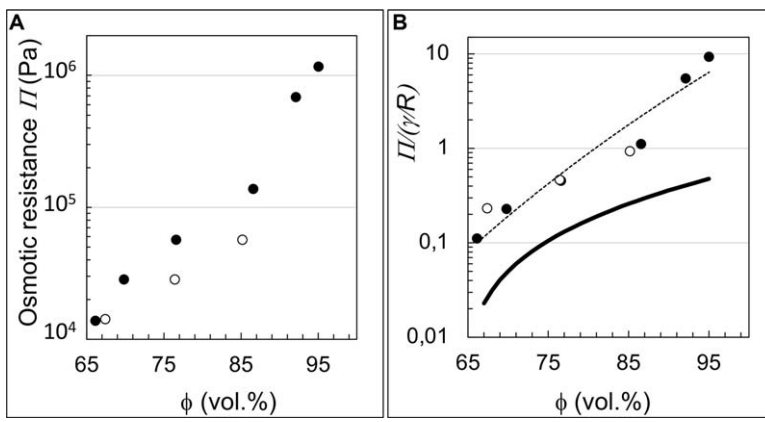

Figure 1.5 (A) Evolution of the osmotic resistance, Π, as a function of the droplet volume fraction ϕ for hexadecane-in-water emulsions. Open circles: $d_{32} = 0.49$ μm; full circles: $d_{32} = 0.24$ μm. (B) Evolution of the osmotic resistance, Π, normalized by γ/R. The dashed line just follows the trend of the experimental data. The solid line corresponds to eqn (1.5).

dependence on the oil volume fraction, when scaled with the Laplace pressure of the non-deformed droplets, γ/R:[25]

$$\Pi/\left(\frac{\gamma}{R}\right) \approx G'/\left(\frac{\gamma}{R}\right) \approx 1.7\phi^2(\phi - \phi^*) \quad (1.5)$$

The scaling with γ/R confirms that the elasticity and osmotic pressure of monodisperse emulsions depend only on the packing geometry of the compressed droplets and on Laplace pressure. In principle, it is necessary to consider the effective oil volume fraction in order to account for the repulsive interactions between the droplets. As highlighted by Princen *et al.*,[26] the effective oil volume fraction, ϕ_{eff}, integrates the thickness, h, of the thin films between the deformed droplets:

$$\phi_{\text{eff}} = \phi\left(1 + \frac{h}{d_{32}}\right)^3 \quad (1.6)$$

It is reasonable to assume that h is comparable to the protein size, *i.e.*, a few nanometers. For the emulsions that were probed, the droplet diameter ($d_{32} > 0.25$ μm) was very large compared to the protein size. Since $h/d_{32} < 5{\cdot}10^{-2}$, the corrective term in eqn (1.6) was neglected and the effective droplet volume fraction was assumed to be equal to the actual oil volume fraction, ϕ.

In Figure 1.5B, we report the evolution of the osmotic resistance normalized by γ/R, with $\gamma = 15$ mN m^{-1} (Section 1.2.3.5). The data fall onto a single curve within reasonable experimental uncertainty. Our results were compared to the normalized data obtained by Mason *et al.*[25] for emulsions stabilized by a low molecular-weight surfactant (SDS). The latter are represented as a solid line which corresponds to the best fit to the experimental points given by eqn (1.5). It clearly appears that the obtained values for protein-stabilized emulsions are much higher than the ones obtained in the presence of surfactant. This behavior indicates that, in our case, droplet deformability is not determined by surface tension. Dimitrova and Leal-Calderon[27] have measured $\Pi(\phi)$ and $G'(\phi)$ for hexadecane-in-water emulsions stabilized by proteins of animal origin. They found that emulsions stabilized by globular proteins like bovine serum albumin (BSA), β-lactoglobulin (BLG), or lysozyme possess remarkably high elasticity and osmotic resistance in comparison with equivalent emulsions stabilized by surfactants. They argued that this behavior may have two different origins: (i) adhesion or stickiness of the protein-stabilized films and (ii) viscoelasticity of the protein interfacial layers. Actually, the two factors cannot be considered separately, because both arise from specific interactions between the adsorbed proteins and are intrinsically interrelated.

It is widely accepted that proteins stabilize the emulsions, forming a viscoelastic film at the interface.[28] A protein layer can be considered as a two-dimensional body, which has its own rheological properties.[29,30]

The interfacial concentration is of the order of several $mg\,m^{-2}$,[31] and this was confirmed by the interfacial coverages measured in Section 1.3.2. The adsorption of proteins is generally followed by gradual unfolding. In this process, proteins lose their secondary and higher structure in the adsorbed state. Unfolding uncovers different segments of adsorbed species, which facilitates lateral interactions of various types between the adsorbed molecules: ionic, hydrophobic, covalent (disulfide bridging), or hydrogen bonding. As a result, the adsorbed protein layers are viscoelastic, and almost tangentially immobile.[32,33] This is especially true for globular proteins like BLG, which can form disulfide bridges[34] and lead to a cohesive elastic network within the interface.[35]

Useful information concerning the properties of protein-stabilized emulsions can be obtained from model experiments on thin liquid films using a Scheludko-type cell.[36] Dimitrova and Leal-Calderon[27] performed this type of experiment with globular proteins in order to mimic the films present in concentrated emulsions. Films stabilized by BSA and BLG were found to aggregate forming rigid clusters that joined the interfaces and rigidified them. Dynamic light scattering from bulk solutions of BSA and BLG revealed no clustering in bulk solutions, while large aggregates at the surface were clearly observed during thin liquid film studies, most probably due to extensive interfacial protein unfolding.[37,38]

The same type of behavior has been found in emulsions stabilized by solid particles. Arditty *et al.*[39] measured the bulk properties of solid-stabilized concentrated emulsions and deduced some characteristic properties of the interfacial layers covering the droplets. The osmotic resistance, Π, of the emulsions was measured for different oil volume fractions above $\phi^{\star}$. The dimensionless osmotic pressure, $\Pi/(\gamma/R)$, was always substantially higher than the corresponding values obtained for surfactant-stabilized emulsions. The authors concluded that droplet deformation in solid-stabilized emulsions is not controlled by the capillary pressure, γ/R, of the non-deformed droplets but rather by σ_0/R, with σ_0 being a parameter characterizing the rigidity of the droplet surfaces induced by the very strong lateral interactions between the solid particles adsorbed at the interface. Their data were interpreted considering that the interfacial layers are elastic at small deformations and exhibit plasticity at intermediate deformations. σ_0 corresponds to the surface yield stress, *i.e.,* the transition between elastic and plastic regimes.

1.3.4 Macroscopic Aspect of Concentrated Emulsions as a Function of the Droplet Fraction – Biliquid Foams

Hexadecane-in-water emulsions were submitted to centrifugation until a dense cream was formed and the subnatant phase was fully transparent (Figure 1.6A). After centrifugation, the creams were collected and dried to estimate their droplet fraction. Figure 1.6B shows the macroscopic aspect of an emulsion whose droplet fraction is close to 75 vol%. The sample resembles a solid paste that sustains its own weight. The sample exhibits a smooth texture and is

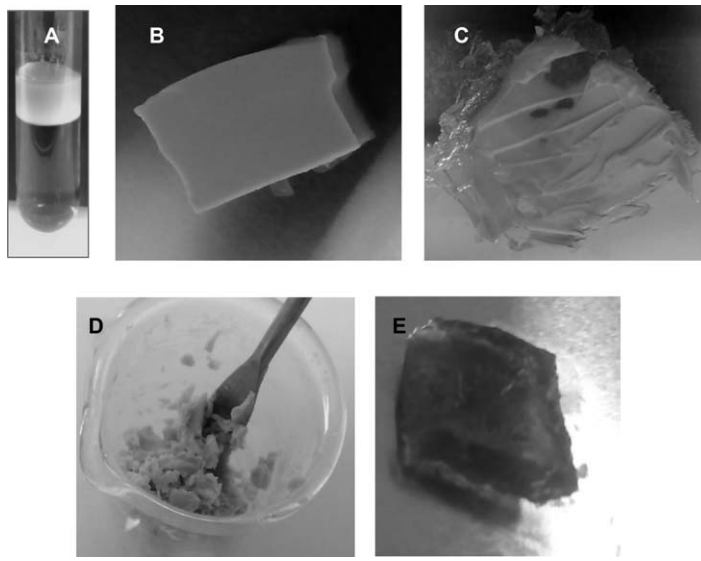

Figure 1.6 Hexadecane-in-water materials obtained by centrifugation (1 wt% proteins) and/or water evaporation. (A) Emulsion in the centrifuge tube; (B) and (C) Emulsions with 75% volume fraction; (D) Emulsions with 90% volume fraction; (E) Biliquid foam (~99 vol%).

spreadable upon application of shear, as illustrated in Figure 1.6C. At higher droplet fractions, of the order of 90 vol%, corresponding to larger acceleration rates in the centrifuge, the dense emulsions became brittle materials. They readily disintegrated into small pieces when they were manipulated. A photograph revealing this behavior is shown in Figure 1.6D. Such brittleness is the reason why rheological measurements were not performed, as it was not possible to load the sample cell properly at high droplet fractions. Osmotic resistance measurements were carried out preferentially, bearing in mind that Π and G' have been found to have comparable values in emulsions stabilized by surfactants[25] and solid particles.[39]

Some samples were allowed to evaporate for at least 24 hours after centrifugation. The evaporation of water led to the formation of a transparent solid-like material (Figure 1.6E) that contained about 99% of dry extract (oil + protein). Furthermore, within experimental error, the sample mass remained constant over several days. These observations provide evidence that almost all of the water content evaporated. In this case, droplets are expected to become polyhedral and these concentrated materials are referred to as ''biliquid foams''. They are the kinds of solids which, on gentle touch, exhibit a strong elastic response. However, they are fragile: at strong deformation, they release oil. The same observations were obtained with rapeseed-in-water emulsions (data not shown).

Biliquid foams based on low molecular-weight surfactants generally release oil when the stabilizing layers are dehydrated by free evaporation.[40]

On the contrary, our biliquid foams withstand evaporation without being destroyed. They exhibit remarkable resistance to coalescence. This property probably arises from the specific nature of the interfacial layers comprising unfolded proteins which are sufficiently thick and rigid to protect the globules against coalescence. It is worth noticing that this type of material has already been obtained in the presence of BSA and BLG.[27] Our results thus generalize the concept of using globular proteins that undergo interfacial unfolding to obtain emulsions with outstanding stability.

1.3.5 Emulsions Concentrated by Freeze-drying

Compared to conventional emulsions, dry emulsions have many technological assets: increased shelf life, lack of bacteriological growth owing to the very low water activities, facilitated transport, and improved oil stabilization against oxidation.[41–43] We implemented freeze drying as a means to obtain concentrated emulsions starting from dilute ones. Freeze drying induces cryo-concentration of the droplets, likely to compress them and to provoke coalescence.[44] To avoid oil droplets from merging into a macroscopic separated oil phase, either during the drying process or during the storage of the dry powder, a hydrophilic wall material is generally added to the aqueous phase. Typical examples of species used as wall materials are glucose, lactose, maltodextrin, starch, and cellulose. Once water is evaporated, this wall material, together with the emulsifier used to stabilize the emulsion, forms a solid phase that surrounds the droplets, thus avoiding their recombination (coalescence). The required amount of solid wall material generally varies from 30 to 80 wt% of the total final powder.[41]

Freeze-drying was implemented as described in Section 1.2.3.6 to dehydrate rapeseed O/W emulsions. The final dried systems were obtained in powder form. Parent emulsions were formulated in the presence of 3 saccharides: trehalose, mannitol, and lactose. Their aqueous phase initially contained 2 wt% of SP and 20 wt% of saccharide. The redispersible capacity of the powders in water was examined following the protocol described in Section 1.2.3.8. The behavior of emulsions containing wall material was compared to a control system devoid of saccharide.

After freeze-drying, the obtained powders contained about 53 wt% of rapeseed oil, 42 wt% of saccharide, 4 wt% of SP, and 1% of residual moisture. The powder deriving from the control system contained 92 wt% of rapeseed oil, 7 wt% of SP, and 1% of moisture. Irrespective of the saccharide nature, the moisture content was close to 1 wt%, within the prescribed regulations for dried powder in the food industry (<3–4 wt%).[41] The powders remained kinetically stable under quiescent conditions in sealed bags, with no apparent macroscopic oil leakage even after several months of storage at room temperature, reflecting efficient stabilization of the oil droplets by the solid component. However, the control system and the powder based on mannitol were clearly clumpier and greasier. Figure 1.7 shows the visual macroscopic aspect, as well as typical micrographs of the systems.

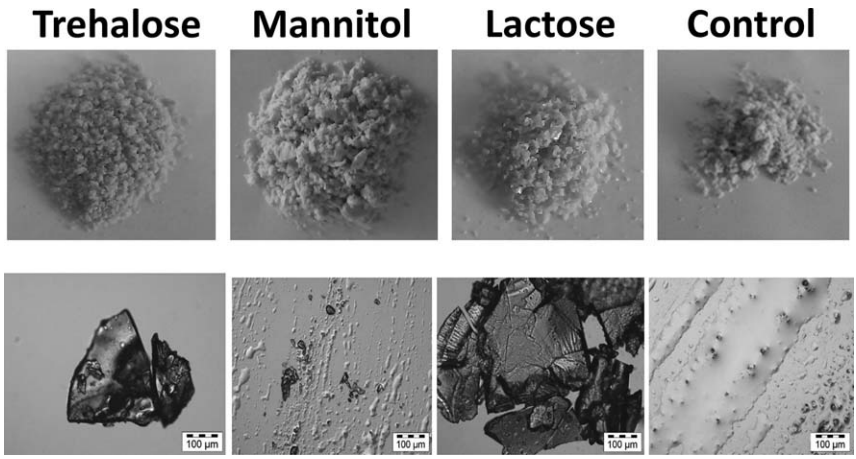

Figure 1.7 Morphologies of freeze-dried rapeseed oil-in-water emulsions containing different saccharides as wall material. The control system was devoid of saccharide. Top: Macroscopic aspect; Bottom: Micrographs.

Dry emulsions are made of large (>10 μm) irregularly shaped and aggregated solid grains. To carry on the observations with the microscope, powders were forced to spread on the glass slide with a spatula and it is apparent that free oil is present around the grains and wets the glass substrate in both the emulsion containing mannitol and in the control.

Powders were rehydrated the same day using pure water in order to restore the composition of the parent emulsions (method described in Section 1.2.3.8). To assess the ability of the drying process to preserve the state of dispersion, the size distributions of the oil droplets were compared before dehydration and after redispersion of the powders in an aqueous phase. Data are gathered in Figure 1.8 (A: size distributions; B: micrographs). Regardless of the presence or absence of wall material and of the saccharide nature, the average droplet size of parent emulsions is close to 0.25 μm and the droplet size distribution is quite narrow, with $P < 0.51$. All rehydrated emulsions have a size distribution broader than the one corresponding to their parent emulsion (the polydispersity index P is always larger than the initial one), reflecting partial droplet coalescence induced by the freeze-drying process. In the control system and in the emulsion based on mannitol, the peak of the initial droplet size has almost fully disappeared, at the expense of a mode between 10 and 100 μm. Thus, the emulsion droplets have undergone significant coalescence during freeze-drying. The size distributions are in accord with the greasy aspect of the powder and with the micrographs of Figure 1.7. Conversely, trehalose and lactose provide a good level of protection against coalescence. The intensity of the mode located between 0.1 and 1 μm remains significant, and the shoulder observed at larger sizes induced by coalescence represents less than 25% of the droplets volume (cumulated fraction). It is within the scope of future work to analyze

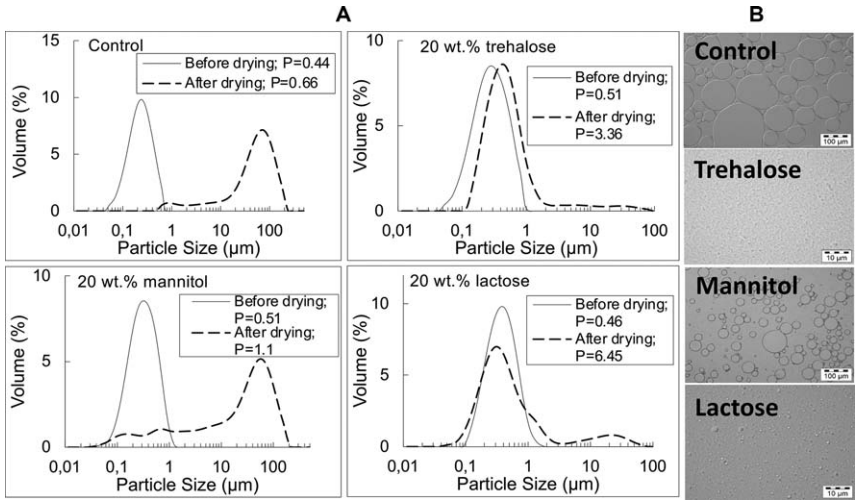

Figure 1.8 (A) Size distributions of parent and rehydrated emulsions for rapeseed oil-in-water emulsions containing different saccharides as wall materials. (—) Parent emulsion; (– – –) Rehydrated emulsion after freeze-drying. (B) Micrographs of rehydrated emulsions.

dehydrated emulsions by spray drying, a process that generally reduces the extent of droplet coalescence.[45]

To sum up, our results reveal that emulsions processed by freeze-drying are more prone to coalescence than those submitted to centrifugation and/or simple evaporation at room temperature that were described in Section 1.3.4. However, whatever the technique used to concentrate the emulsions, bulk or powdered solid materials can be obtained with no macroscopic oil leakage at rest.

1.4 Conclusions

Hydrophilic biopolymers like proteins or polysaccharides provide the chemical ''scaffold'' to produce water-based gels. Since they are insoluble in oil, finding a way to make them oil gelators would considerably expand their applications field. In this chapter, we have reported an approach to generate oleogels containing liquid oil and hydrophilic biopolymers. The approach is simple, versatile and is based on the preparation of a fine O/W emulsion, followed by removal of the water phase, resulting in the physical trapping of oil droplets in a protein network. A large variety of textures could be achieved by varying the droplet fraction: viscous fluids, viscoelastic pastes, and elastic ''gums'' (transparent biliquid foams), as ϕ increased from 65 to 99 vol%. Drying concentrated emulsions usually provokes coalescence of the oil droplets, resulting in the full separation of the two immiscible phases. This instability can be prevented if the droplet interface is stiffened. The concept of structuring liquid oils by using O/W emulsions as templates was first

reported by Gao *et al.*[46] and by Romoscanu and Mezzenga.[47] In their cases, stabilization was achieved by either forming surfactant–protein complexes[46] or by crosslinking proteins at the oil–water interface with chemicals.[47] Patel *et al.*[5] found a route for emulsion stabilization without the need for any surfactant or a crosslinking step. Stabilization was obtained with only a combination of polysaccharides. Here, we went on step further by using solely globular proteins that deliver interfacial stiffness owing to unfolding. Following a previous work on concentrated emulsions stabilized by animal proteins,[24,27] vegetal proteins were used as emulsion stabilizers to build up solid properties while preserving the low viscosity and ease of manufacturing. This kind of system can find applications in food matrices that require texturized oils. They can be easily handled at room temperature at a volume fraction such that they remain easily spreadable (<75%), and then *in situ* evaporation transforms them into solids. Finally, we could formulate dried-emulsions in powder form after submitting initial dilute emulsions to a freeze-drying step in the presence of a wall material (saccharide). Advantageously, the obtained powders were fully redispersible in water.

Acknowledgements

This study was performed in partnership with the French Institute for the Energy Transition (Institut pour la Transition Energétique) PIVERT (www.institut-pivert.com) and supported by the French Government under the reference ANR-001-01. Alexandre Poirier, Laurence Ramos, Amélie Blanc, and Martin In are gratefully acknowledged for fruitful discussions.

References

1. R. Uauy, A. Aro, R. Clarke, M. R. L'Abbé, D. Mozaffarian, C. M. Skeaff, S. Stender and M. Tavella, *Eur. J. Clin. Nutr.*, 2009, **63**, S68.
2. https://www.who.int/news/item/14-05-2018-who-plan-to-eliminate-industrially-produced-trans-fatty-acids-from-global-food-supply (last accessed January 2021).
3. S. S. Narine and A. G. Marangoni, *Food Res. Int.*, 1999, **32**(4), 227.
4. A. Bot, R. den Adel and E. C. Roijers, *J. Am. Oil Chem. Soc.*, 2008, **85**, 1127.
5. A. R. Patel, N. Cludts, M. D. Bin Sintang, B. Lewille, A. Lesaffer and K. Dewettinck, *Chem. Phys. Chem.*, 2014, **15**(16), 3435.
6. H. M. Princen, *J. Colloid Interface Sci.*, 1983, **91**, 160.
7. T. G. Mason, A. H. Krall, H. Gang, J. Bibette and D. A. Weitz, in *Encyclopedia of Emulsion Technology*, ed. P. Becher, Marcel Dekker, New York, 1996, vol. 4, p. 299 and references therein.
8. W. Dridi, C. Harscoat-Schiavo, J. Monteil, C. Faure and F. Leal-Calderon, *Langmuir*, 2018, **34**, 9228.
9. S. Gonzalez-Perez and J. M. Vereijken, *J. Sci. Food Agric.*, 2007, **87**, 2173.
10. J. Kjeldahl, *Z. Anal. Chem.*, 1883, **22**(1), 366.

11. E. Layne, in *Method in Enzymology*, ed. P. S. Colowick and N. O. Kaplan, Academic Press, Inc., New York, 1957, vol. 3, p. 447.
12. R. A. Y. Haar, R. D. Allen, E. A. Cohen, C. L. Nessler and T. L. Thomas, *Gene*, 1988, **74**(2), 433.
13. M. Dalgalarrondo, J. Raymond and J.-L. Azana, *J. Exp. Bot.*, 1984, **35**(11), 1618.
14. A. A. Kortt and J. B. Caldwell, *Phytochemistry*, 1990, **29**(5), 1389.
15. A. A. Kortt and J. Caldwell, *Phytochemistry*, 1990, **29**(9), 2805.
16. J. Raymond, J. M. Robin and J. L. Azanza, *Plant Syst. Evol.*, 1995, **198**(3), 195.
17. I. N. Anisimova, R. J. Fido, A. S. Tatham and P. R. Shewry, *Euphytica*, 1995, **83**(1), 15.
18. S. Gonzalez-Perez and J. M. Vereijken, *J. Sci. Food Agric.*, 2007, **87**, 2173.
19. A. Poirier, *Propriétés fonctionnelles de protéines végétales, en volume et aux interfaces fluides*, PhD thesis, 2019, University of Montpellier.
20. D. Karefyllakis, S. Altunkaya, C. C. Berton-Carabin, A. J. van der Goot and C. V. Nikiforidis, *Food Hydrocolloids*, 2017, **73**, 326.
21. P. Plietz, G. Damaschun, J. J. Muller and K. D. Schwenke, *Eur. J. Biochem.*, 1983, **130**, 315.
22. G. Mie, *Ann. Phys.*, 1908, **330**(3), 377.
23. M. M. Bradford, *Anal. Biochem.*, 1976, **72**, 248.
24. T. D. Dimitrova and F. Leal-Calderon, *Adv. Colloid Interface Sci.*, 2004, **108–109**, 49.
25. T. M. Mason, J. Bibette and D. A. Weitz, *Phys. Rev. Lett.*, 1995, **75**, 2051.
26. H. M. Princen, M. P. Aronson and J. C. Moser, *J. Colloid Interface Sci.*, 1980, **75**, 246.
27. T. D. Dimitrova and F. Leal-Calderon, *Langmuir*, 2001, **17**, 3235.
28. E. Dickinson and A. Williams, *Colloids Surf.*, 1994, **88**, 317.
29. E. Lucassen-Reynders and J. Benjamins, in *Food Emulsions and Foams Interfaces, Interactions and Stability*, ed. E. Dickinson and J. M. Rodriguez Patino, Royal Society of Chemistry, London, 1999, p. 195.
30. D. E. Graham and M. C. Phillips, *J. Colloid Interface Sci.*, 1979, **70**, 415.
31. S. Tcholakova, N. D. Denkov, I. B. Ivanov and B. Campbell, *Langmuir*, 2002, **18**(23), 8960.
32. M. A. Bos and T. van Vliet, *Adv. Colloid Interface Sci.*, 2001, **91**(3), 437.
33. E. M. Freer, K. S. Yim, G. G. Fuller and C. Radke, *J. Phys. Chem. B*, 2004, **108**(12), 3835.
34. E. Dickinson and Y. Matsumura, *Int. J. Biol. Macromol.*, 1991, **13**(1), 26.
35. A. Williams and A. Prins, *Colloids Surf., A*, 1996, **114**, 267.
36. A. Scheludko, *Kolloid-Z*, 1957, **155**, 39.
37. T. D. Dimitrova, *Emulsions stabilisées par les protéines: forces collóîdales, rhéologie et crémage*, PhD thesis, University of Bordeaux, Bordeaux, France, 2000.
38. T. G. Gurkov, K. G. Marinova, A. Z. Zdravkov, C. Oleksiak and B. Campbell, *Prog. Colloid Polym. Sci.*, 1998, **110**, 263.

39. S. Arditty, F. Lequeux, V. Schmitt and F. Leal-Calderon, *Eur. Phys. J. B*, 2005, **44**, 381.
40. O. Sonneville-Aubrun, V. Bergeron, T. Gulik-Krzywicki, B. Jonsson, H. Wennerström, P. Linder and B. Cabane, *Langmuir*, 2000, **16**, 1569.
41. Y. S. Gu, E. A. Decker and D. J. McClements, *J. Agric. Food Chem.*, 2004, **52**(11), 3626.
42. U. Klinkesorn, P. Sophanodora, P. Chinachoti, D. J. McClements and E. A. Decker, *J. Agric. Food Chem.*, 2005, **53**(21), 8365.
43. L. A. Shaw, D. J. McClements and E. A. Decker, *J. Agric. Food Chem.*, 2007, **55**(8), 3112.
44. A. Marefati, M. Rayner, A. Timgren, P. Dejmek and M. Sjöö, *Colloids Surf., A*, 2013, **436**, 512.
45. C. Joseph, R. Savoire, C. Harscoat-Schiavo, D. Pintori, J. Monteil, C. Faure and F. Leal-Calderon, *LWT-Food Sci. Technol.*, 2019, **113**, 108311.
46. Z.-M. Gao, X.-Q. Yang, N.-N. Wu, L.-J. Wang, J.-M. Wang, J. Guo and S.-W. Yin, *J. Agric. Food Chem.*, 2014, **62**, 2672.
47. A. I. Romoscanu and R. Mezzenga, *Langmuir*, 2006, **22**, 7812.